

*Уточнена математична модель кабельного відгалуження перетворювача частоти у складі електромережі дільниці шахти при однофазному замиканні на землю. Модель враховує дискретний характер вихідної напруги та інерційність комутації силових ключів інвертора напруги у складі перетворювача. Запропонована методика формування математичної моделі кабельної лінії з розподіленими параметрами як сукупності диференціальних рівнянь стану та алгебраїчних рівнянь зв'язку у матричній формі. При цьому кабель розбивається на трифазні елементарні секції, для сукупності типових схем заміщення яких будується граф, розраховуються матриця головних перетинів та матричні коефіцієнти рівнянь. Розв'язання останніх виконується чисельними методами. Це дозволяє врахувати хвильові процеси в кабелі при дії високочастотної широтно-імпульсно модульованої вихідної напруги перетворювача частоти. Також враховується несиметрія активних опорів ізоляції відносно землі, що супроводжує замикання на землю. Застосування матрично-топологічного підходу дозволяє уникнути операцій з частинними похідними по геометричним координатам кабелю. Актуальність досліджень обумовлена нехтуванням у відомих моделях суттєвими факторами, що знижує точність аналізу. Зокрема, не беруться до уваги вплив на миттєві значення струму замикання дискретного характеру напруги на виході перетворювача частоти, розподілений характер параметрів ізоляції кабельної лінії та поперечна несиметрія в аварійному режимі. В результаті чисельного моделювання для конкретної мережі встановлено, що виникнення замикання на землю через тіло людини в кабельному відгалуженні перетворювача частоти характеризується неприпустимо великою імовірністю смертельного електроураження. Обґрунтовано спосіб контролю активного опору ізоляції відгалуження електричної мережі з напівпровідниковим перетворювачем частоти. Реалізація способу дозволить підвищити електробезпеку підземних електричних мереж за рахунок своєчасного виявлення ушкодження ізоляції кабельного відгалуження перетворювача частоти і передачі сигналу на відключення напруги*

*Ключові слова: перетворювач частоти, замикання на землю, автономний інвертор, змінні стану, електроураження*

UDC 621.341.572:621.315.2.016.2  
DOI: 10.15587/1729-4061.2019.176571

# REFINEMENT OF THE MATHEMATICAL MODEL OF FREQUENCY CONVERTER CABLE BRANCH WITH A SINGLE-PHASE SHORT CIRCUIT

**S. Vasylets**

Doctor of Technical Sciences,  
Associate Professor\*

E-mail: svyat.vasilets@gmail.com

**K. Vasylets**

Assistant\*

E-mail: k.s.vasylets@nuwm.edu.ua

\*Department of Automation, Electrical  
Engineering and Computer-Integrated  
Technologies

National University of Water and  
Environmental Engineering

Soborna str., 11, Rivne, Ukraine, 33028

Received date 30.06.2019

Accepted date 01.08.2019

Published date 28.08.2019

Copyright © 2019, S. Vasylets, K. Vasylets

This is an open access article under the CC BY license

(<http://creativecommons.org/licenses/by/4.0>)

## 1. Introduction

A large number of frequency converters (FC) for induction electric drives are operating as a part of underground mine power networks nowadays. In particular, to control the speed of belt conveyors the PChV-K U5 converters are used, of underground lifting machines – PChV-250 U5. The coal combines of UDK400, KDK500 types with a frequency-controlled drive are also used. The high probability of damaging the insulation of a flexible cable, which connects the motor to the FC, causes the risk of ground fault. This can result in an electric injury to a person. The probability of explosion of methane-air mixture, caused by the electric arc, is also high.

Methods of ground fault protection in networks with grounded neutral point have proven to be effective [1]. The neutral point of underground power grids in Ukraine is isolated. This complicates the detection of ground fault in

the FC cable branches. The protection device AZUR-4pp has been developed for the combined power networks of coal mines. The disadvantage of this device consists in using the direct current, which is overlaid on the common part of the network, to control the isolation level of the FC cable branch. This principle is characterized by low reliability, especially when the FC is in pulse-width modulation (PWM) mode of the output voltage.

The urgency of increasing the electrical safety of FC operation is caused by the high probability of cable lines damage in the combined underground power networks and by the drawbacks of the existing protection devices. This can be achieved by refinement of the mathematical model of the FC cable branch in a network with the isolated neutral point. The model should take into account the operation peculiarities of the “semiconductor converter – long cable line” system in the asymmetrical mode of single-phase ground fault.

---

## 2. Literature review and problem statement

---

Studies of ground fault in the FC cable branch are most often limited by the use of simplified models. Considering the parameters of cable insulation by the lumped capacitances is typical [2]. This does not allow to take fully into account the influence of higher harmonics of the FC output voltage on the state of the single-phase short circuit. The discrete nature of the FC output voltage is also disregarded [3].

Methods of studying transients in long power lines in normal and emergency modes are divided into two main groups. The first group includes methods that involve models with distributed parameters. The mathematical description of the line is based on known telegraph equations. Solving such equations of state in partial derivatives by the finite element method for a particular time moment provides the highest accuracy of the analysis [4]. However, these equations can hardly be solved using numerical methods over a given time interval. The methods of the second group, in particular, the finite section method, represent each phase of a long cable line by the sequential connection of elementary sections with constant parameters [5]. The scope of this approach is limited by the case of phase symmetry of the elementary sections impedance. The ground fault occurrence violates the symmetry, which cannot be properly taken into account. To determine the dependence of the long lines parameters on the voltage frequency, the sub-conductor method [6] can be used, which takes into account the skin effect and the proximity effect in the core.

The “Three-Phase PI Section Line” and “Distributed Parameter Line” Simulink blocks of the SimPowerSystems library are used to model long power lines. The first of these blocks represents one elementary section of a three-phase line with lumped parameters. The second block simulates a multiphase power line with distributed parameters. The main disadvantage of these blocks lies in neglect of the line-to-ground resistance of insulation. This drawback makes it impossible to use these blocks for exploring the ground fault in the FC cable branch because of significant errors in the calculations.

The inability to determine the impedance of the phase-to-ground short circuit at the FC output if the protective device is connected in the common part of the network complicates the construction of protection devices [7]. Erroneous operation of regular ground fault protection devices can also be caused by the semiconductor converter as a part of the mine section electrical network [8].

The consequences of electrocution significantly depend on the frequency of the current through the human body [9]. In particular, the harmonic composition of the short circuit current depends on the PWM frequency of the converter, the angular speed of the motor and the parameters of the FC output filter, as it was found in [10]. This work also found that higher-order harmonics pose less danger to humans than low-frequency components. The effect of polyharmonic current on the human body in the IEC 60479-2 standard is recommended to evaluate by a value of an equivalent current  $I_B$  at industrial frequency. It is possible to estimate the electrical safety of the short circuit through the human body by the  $I_B$  value using the probabilistic electrical characteristics given in the IEC 60479-1 standard.

Thus, the efficiency of the existing ground fault protection devices is reduced by the frequency converters in the mine section electrical network [11]. Known mathematical

models are characterized by insufficient accuracy due to the neglect of essential factors. This causes the statement of the scientific and technical problem that consists in increasing the electrical safety in underground combined networks. A solution to this problem is to refine the mathematical model of the frequency converter cable branch with a single phase-to-ground fault. Improving the accuracy of the simulation is possible by taking into account the discrete nature of the voltage, distributed parameters of the cable and the significant asymmetry that accompanies the specified emergency mode. This will allow a more accurate probability assessment of a person fatal electrocution in the underground power network of specific configuration. It will also be possible to determine the advisability of equipping the FC cable branch with a protective apparatus under the specified conditions. The simulation results can be used to ground the requirements for advanced protection devices. In particular, the maximum permissible time of the network protective shutdown can be estimated.

---

## 3. The aim and objectives of the study

---

The aim of the study is to refine the mathematical model of the FC cable branch with a single phase-to-ground fault, which will enable to increase the electrical safety of underground electrical networks.

To achieve the set aim, the following objectives must be accomplished:

- to improve the mathematical model of an autonomous voltage inverter as the FC part, taking into account the inertia of the driver circuit and the transient process of the power semiconductor devices switching;
- to refine the mathematical model of the three-phase power cable branch, as an object with distributed parameters, of the frequency converter taking into account the transverse asymmetry in the case of single phase-to-ground fault;
- to substantiate the structure of the FC cable branch computer model in the case of ground fault;
- to formulate practical recommendations for increasing the electrical safety of underground electrical networks equipped with frequency converters;
- to estimate the probability of a person fatal electrocution based on the results of the analysis of single phase-to-ground fault simulation in the FC cable branch for the electrical network of a specific configuration.

---

## 4. Mathematical model of the autonomous voltage inverter

---

The frequency converter with a direct current link consists of a rectifier, a filter and an autonomous voltage inverter (AVI). Further studies are concerned with the analysis of the AVI output voltage effect on the phase-to-ground short circuit.

The equivalent circuit (Fig. 1) is used to simulate the AVI. The inverter is powered by an ideal source  $U_d$  of constant electromotive force with internal resistance  $R_d$ . The power transistors are represented by  $R_1$ – $R_6$  resistors, which resistance changes exponentially when switching semiconductor devices. The open state of the transistor corresponds to the  $R_{on}$  resistance, closed –  $R_{off}$ . The time constant  $T$  of

the aperiodic transient of resistance change during switching is determined by the inertia of the driver circuit and the values of the parasitic capacitances of the semiconductor device. A three-phase resistor star  $R_7$ – $R_9$  is connected to the output nodes 2–4 of the inverter, on which the output phase voltages are available.

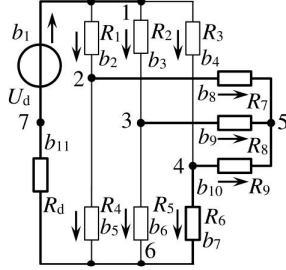


Fig. 1. Equivalent circuit of the autonomous voltage inverter

The equivalent circuit of the inverter is analyzed using the matrix-topological method of the electric circuit analysis. The algorithms [12] for constructing a graph tree of the circuit and a matrix of major cross sections are used.

The graph of the AVI equivalent circuit is formed by the independent source  $U_d$  of electromotive force and the resistive edges  $R_6$ – $R_9$ ,  $R_d$ , indicated in Fig. 1 with thick lines. In this case,  $U_d$  corresponds to the direct voltage of the frequency converter. The Ohm's law in matrix form relates the vectors of currents of resistive edges  $\mathbf{I}_{Red}$  and chords  $\mathbf{I}_{Rch}$  to the corresponding voltage vectors  $\mathbf{U}_{Red}$ ,  $\mathbf{U}_{Rch}$  as follows:

$$\mathbf{I}_{Red} = \mathbf{R}_{ed}^{-1} \cdot \mathbf{U}_{Red}; \quad (1)$$

$$\mathbf{I}_{Rch} = \mathbf{R}_{ch}^{-1} \cdot \mathbf{U}_{Rch}, \quad (2)$$

where  $\mathbf{R}_{ed}$ ,  $\mathbf{R}_{ch}$  – diagonal resistance matrices of resistive edges and chords, respectively, and:

$$\mathbf{R}_{ed} = \text{diag}\{R_6, R_7, R_8, R_9, R_d\}; \quad (3)$$

$$\mathbf{R}_{ch} = \text{diag}\{R_1, R_2, R_3, R_4, R_5\}. \quad (4)$$

The AVI equivalent circuit is described by the system of matrix algebraic equations, compiled according to the first and second Kirchhoff's laws:

$$\begin{cases} \mathbf{I}_{Red} = -\mathbf{F}_{Red,Rch} \cdot \mathbf{I}_{Rch}; \\ \mathbf{U}_{Rch} = \mathbf{F}_{U,Rch}^T \cdot \mathbf{U}_d + \mathbf{F}_{Red,Rch} \cdot \mathbf{U}_{Red}, \end{cases} \quad (5)$$

where  $\mathbf{F}_{U,Rch}$ ,  $\mathbf{F}_{Red,Rch}$  – the submatrices of the major cross sections matrix of the AVI equivalent circuit graph, which connect the independent voltage sources and resistive chords, and the resistive edges and chords, respectively, and:

$$\mathbf{F}_{U,Rch} = [1 \ 1 \ 1 \ 0 \ 0]; \quad (6)$$

$$\mathbf{F}_{Red,Rch} = \begin{bmatrix} -1 & -1 & -1 & 1 & 1 \\ -1 & 0 & 0 & 1 & 0 \\ 0 & -1 & 0 & 0 & 1 \\ 1 & 1 & 0 & -1 & -1 \\ -1 & -1 & -1 & 0 & 0 \end{bmatrix}. \quad (7)$$

Taking into account equations (1), (2) in the system (5), the matrix equation can be obtained that allows to calculate the voltage vector  $\mathbf{U}_R = [\mathbf{U}_{Red} \ \mathbf{U}_{Rch}]^T$  on the resistive elements of the AVI equivalent circuit:

$$\mathbf{U}_R = L_1^{-1} \cdot L_2 \cdot \mathbf{U}_d, \quad (8)$$

where  $L_1$ ,  $L_2$  – matrix coefficients that are:

$$L_1 = \begin{bmatrix} \mathbf{R}_{ed}^{-1} & \mathbf{F}_{Red,Rch} \cdot \mathbf{R}_{ch}^{-1} \\ -\mathbf{F}_{Red,Rch}^T & \mathbf{E} \end{bmatrix}; \quad (9)$$

$$L_2 = [\mathbf{Z} \ \mathbf{F}_{U,Rch}^T]^T, \quad (10)$$

and  $\mathbf{E}$ ,  $\mathbf{Z}$  – single and zero matrices, respectively.

Thus, the obtained matrix algebraic equation (8) is the mathematical model of the autonomous voltage inverter. The output phase voltages of the inverter  $u_a$ ,  $u_b$ ,  $u_c$  correspond to the voltages at resistors  $R_7$ ,  $R_8$ ,  $R_9$ , i. e. elements of the  $\mathbf{U}_R$  vector with numbers 2, 3, 4.

## 5. Refinement of the mathematical model of the three-phase power cable branch of the frequency converter

The equivalent circuit of the cable line that connects the load to the output of the AVI as a part of the FC is shown in Fig. 2. The voltage sources  $u_a$ ,  $u_b$ ,  $u_c$  correspond to the voltage system at the inverter output. The cable is represented by a set of elementary sections  $K_j$ , and  $j = \overline{1, N}$ . Each section is characterized by the length of  $\Delta l$ . This allows to analyze the cable line as an object with distributed parameters. The cable supplies power to the active-inductive three-phase load, which is connected according to the “star” configuration:  $R_{l\zeta}$ ,  $L_{l\zeta}$ , and  $\zeta = \{a, b, c\}$  is the phase designation.

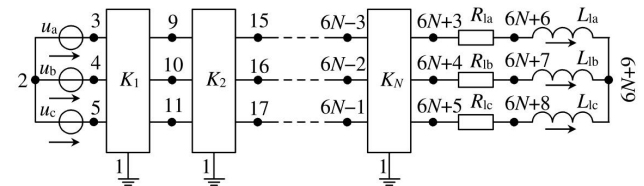


Fig. 2. Equivalent circuit of the distributed cable line with active-inductive load

The equivalent circuit of the three-phase section  $K_j$  of the cable line (Fig. 3) takes into account the resistances ( $R_{c\zeta j}$ ) and inductances ( $L_{c\zeta j}$ ) of the conductors, as well as the resistances ( $R_{g\zeta j}$ ) and capacitances ( $C_{g\zeta j}$ ) of the  $\Delta l$  long cable section insulation. The single phase-to-ground fault at a certain point of the cable line implies a discrete change in the insulation phase-to-ground resistance of a given phase of the cable in the corresponding elementary section. This resistance is supposed to be reduced to the short circuit value, for example, to the resistance of a human body in case of studying the corresponding emergency mode.

The utilization of the matrix-topological method to analyze processes in a distributed cable line arises from the possibility of taking into account significant factors. In particular, insulation phase-to-ground resistance, unlike existing computer models, for example – Simulink-blocks “Three-Phase PI Section Line” and “Distributed Parameter

Line". This method also allows to consider the asymmetry of the line in case of single phase-to-ground fault.

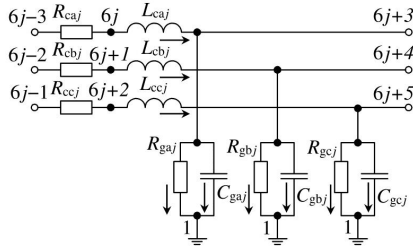


Fig. 3. Equivalent circuit of the three-phase section  $K_j$  of the cable line with distributed parameters

According to the matrix-topological method, a unique number is assigned to each node of the equivalent circuit. No. 1 is assigned to the “ground” contour, No. 2–5 – to the three-phase power source (Fig. 2). The node numbers of the elementary section  $K_j$  of the cable depend on the section number  $j$ , as shown in Fig. 3. The node numbers of the load depend on the total number  $N$  of elementary sections (Fig. 2). The total number of nodes of the distributed cable line equivalent circuit is  $6N+9$ .

For the considered equivalent circuit of the cable line, a graph is constructed and a matrix  $\mathbf{F}$  of major cross sections is formed. The size of the latter is determined by the number  $N$  of cable sections. Generally, the matrix of major cross sections is equal to:

$$\mathbf{F} = \begin{matrix} & \begin{matrix} \{R_{ch}\} & \{L_{ch}\} \end{matrix} \\ \begin{matrix} \{U\} \\ \{C_{ed}\} \\ \{R_{ed}\} \\ \{L_{ed}\} \end{matrix} & \begin{matrix} \mathbf{F}_1 & \mathbf{F}_2 \\ \mathbf{F}_3 & \mathbf{F}_4 \\ \mathbf{F}_5 & \mathbf{F}_6 \\ \mathbf{F}_7 & \mathbf{F}_8 \end{matrix} \end{matrix} \quad (11)$$

and the submatrix  $\mathbf{F}_7$  is zero due to the disconnect between inductive edges and resistive chords.

Based on Kirchhoff's laws, matrix equations are compiled to calculate the vectors of currents of resistive edges  $\mathbf{I}_{Red}$  and voltages of resistive chords  $\mathbf{U}_{Rch}$ :

$$\begin{cases} \mathbf{I}_{Red} = -\mathbf{F}_5 \cdot \mathbf{I}_{Rch} - \mathbf{F}_6 \cdot \mathbf{I}_{Lch}; \\ \mathbf{U}_{Rch} = \mathbf{F}_1^T \cdot \mathbf{U} + \mathbf{F}_3^T \cdot \mathbf{U}_{Ced} + \mathbf{F}_5^T \cdot \mathbf{U}_{Red}. \end{cases} \quad (12)$$

Taking into account Ohm's law for resistive edges and chords, the equation that enables to calculate the vector  $\mathbf{I}_R = [\mathbf{I}_{Red} \ \mathbf{I}_{Rch}]^T$  of the resistive elements currents is possible to obtain from (12):

$$\mathbf{I}_R = \mathbf{A}_1^{-1} \cdot (\mathbf{A}_2 \cdot \mathbf{X} + \mathbf{A}_3 \cdot \mathbf{U}), \quad (13)$$

where  $\mathbf{X} = [\mathbf{U}_{Ced} \ \mathbf{I}_{Lch}]^T$  – vector of state variables – voltages on capacitive edges ( $\mathbf{U}_{Ced}$ ) and currents of inductive chords ( $\mathbf{I}_{Lch}$ );  $\mathbf{U} = [u_a \ u_b \ u_c]^T$  – phase voltage vector of the three-phase power source;  $\mathbf{A}_1, \mathbf{A}_2, \mathbf{A}_3$  – matrix coefficients that are:

$$\mathbf{A}_1 = \begin{bmatrix} \mathbf{E} & -\mathbf{F}_5 \\ -\mathbf{F}_5^T \cdot \mathbf{R}_{ed} & \mathbf{R}_{ch} \end{bmatrix}; \quad (14)$$

$$\mathbf{A}_2 = \begin{bmatrix} \mathbf{Z} & -\mathbf{F}_6 \\ \mathbf{F}_3^T & \mathbf{Z} \end{bmatrix}; \quad (15)$$

$$\mathbf{A}_3 = [\mathbf{Z} \ \mathbf{F}_1^T]^T. \quad (16)$$

The system of matrix differential equations relative to the derivatives of state vectors, compiled using the submatrices of the matrix (11) of graph major cross sections, is as follows:

$$\begin{cases} \mathbf{L}_{ch} \frac{d\mathbf{I}_{Lch}}{dt} = \mathbf{F}_2^T \cdot \mathbf{U} + \mathbf{F}_4^T \cdot \mathbf{U}_{Ced} + \mathbf{F}_6^T \cdot \mathbf{U}_{Red} + \\ + \mathbf{F}_8^T \cdot \mathbf{L}_{ed} \cdot \frac{d}{dt}(-\mathbf{F}_8 \cdot \mathbf{I}_{Lch}); \\ \mathbf{C}_{ed} \frac{d\mathbf{U}_{Ced}}{dt} = -\mathbf{F}_3 \cdot \mathbf{I}_{Rch} - \mathbf{F}_4 \cdot \mathbf{I}_{Lch}. \end{cases} \quad (17)$$

After transformations, the matrix differential equation of state of the cable line with the active-inductive load in Cauchy form can be obtained from (17) as follows:

$$\frac{d\mathbf{X}}{dt} = \mathbf{B}_1^{-1} \cdot (\mathbf{B}_2 \cdot \mathbf{I}_R + \mathbf{B}_3 \cdot \mathbf{X} + \mathbf{B}_4 \cdot \mathbf{U}), \quad (18)$$

where  $\mathbf{B}_1 - \mathbf{B}_4$  – matrix coefficients that are:

$$\mathbf{B}_1 = \text{diag}\{\mathbf{C}_{ed} \cdot \mathbf{L}_{ch} + \mathbf{F}_8^T \cdot \mathbf{L}_{ed} \cdot \mathbf{F}_8\}; \quad (19)$$

$$\mathbf{B}_2 = \begin{bmatrix} \mathbf{Z} & -\mathbf{F}_3 \\ \mathbf{F}_6^T \cdot \mathbf{R}_{ed} & \mathbf{Z} \end{bmatrix}; \quad (20)$$

$$\mathbf{B}_3 = \begin{bmatrix} \mathbf{Z} & -\mathbf{F}_4 \\ \mathbf{F}_4 & \mathbf{Z} \end{bmatrix}; \quad (21)$$

$$\mathbf{B}_4 = [\mathbf{Z} \ \mathbf{F}_2^T]^T. \quad (22)$$

The obtained matrix equations (13) and (18) are the mathematical model of the three-phase power cable that feeds active-inductive load as an object with distributed parameters. Applying the matrix-topological approach to the analysis of dynamic processes in the line allows to take into account the essential asymmetry that accompanies single phase-to-ground fault.

Since the capacitances  $C_{g_{cj}}$  of the cable phase insulation during the construction of the graph tree are edges, the parallel active resistances  $R_{g_{cj}}$  of the insulation are chords. This prevents the formation of closed contours in the graph tree, which is prohibited. This circumstance determines the need to change the value of the corresponding element in the matrix  $\mathbf{R}_{ch}$  of resistances of chords when ground fault occurs.

The ground fault current is defined as an element of the resistive elements currents vector  $\mathbf{I}_R$  that corresponds to the current through the insulation phase-to-ground resistance of the elementary section in the damaged cable.

### 6. Substantiation of the computer model structure of the frequency converter cable branch when ground fault

The block diagram of Fig. 4 explains the model structure of the FC branch cable. Block 1 generates modulating voltage  $u_a^*, u_b^*, u_c^*$  of the AVI with amplitude  $U^*$  and frequency  $f$ . The sawtooth reference voltage  $u_{ref}$  of frequency  $f_{ref}$  is formed by generator 2. The three-phase system of modulating voltages and the reference voltage are supplied to the PWM subsystem 3, which generates the control signals

$V_1...V_6$  for the power semiconductor devices. These signals come to the subsystem 4, which calculates the resistances  $R_1...R_6$  of the power transistors. Defined resistances that correspond to the current state of the semiconductor devices are the inputs of the AVI model 5. The latter implements the matrix equation (8) and distinguishes the vector  $\mathbf{U}$  of the inverter output phase voltages from the calculated vector  $\mathbf{U}_R$ . Block 6 solves the matrix differential equation (18) of the cable line state, taking into account the capacitances  $C_g$  of the cable insulation. The specified block calculates the value of the vector  $\mathbf{X}$  of the cable state variables for the current point in time. The said vector comes to the input of block 7 that calculates the resistive elements currents vector  $\mathbf{I}_R$  of the line according to (13). Block 8 detects instantaneous values of ground fault current from  $\mathbf{I}_R$  and calculates the equivalent operating current  $I_B$  across a human body at industrial frequency.

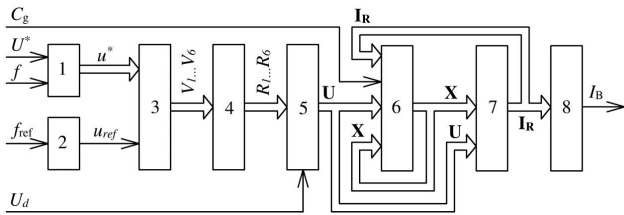


Fig. 4. Generalized block diagram of the model of frequency converter cable branch in case of single phase-to-ground fault

Simulink tools are used to implement the proposed structure of the FC cable branch model. The formation of modulating voltages (Fig. 4, block 1) is carried out by three sinusoidal generators, the output signals of which are connected to the bus (Fig. 5, item 1). The generator (Fig. 4, block 2) of sawtooth reference voltage is implemented by the integrator Integrator1 (Fig. 5, item 6). The following

elements are used to generate PWM control signals (Fig. 4, block 3): null detector (Fig. 5, item 2), which specifies the state of three pairs of corresponding semiconductor devices of the inverter in multiplexed form; inverse elements (Fig. 5, item 3), which divide the control signals into two channels for each pair of semiconductor devices; delay unit (Fig. 5, item 4), which prevents short circuits during switching of each pair of power transistors. The subsystem for calculating the resistances of power transistors (Fig. 4, block 4) sets the resistance value of each of semiconductor devices at the level  $R_{off}=1\text{ M}\Omega$  in the closed state and  $R_{on}=1\text{ m}\Omega$  in the open state (Fig. 5, item 5). The switching inertia of each power device is taken into account by the first-order transfer function (block TF1) with a time constant of  $T=0.2\text{ }\mu\text{s}$ .

The AVI model (Fig. 4, block 5), according to (8), performs the following operations (Fig. 5, item 7). Subsystem1 is used to form diagonal matrices (3), (4) of resistive edges and chords values. Inv blocks provide the calculation of inverse matrices to the specified ones. Subsystem2 performs the formation of the matrix coefficient  $\mathbf{L}_1$  according to (9). The value of the matrix coefficient  $\mathbf{L}_2$  (10) is given by the block L2. The Ud block specifies the voltage  $U_d$  value of the FC direct current circuit. The matrix multiplication unit Matrix Multiply, according to (8), calculates the voltage vector  $\mathbf{U}_R$  on the resistive elements of the AVI equivalent circuit. The Selector block distinguishes the phase output voltages of the AVI.

Numerical solution of the matrix differential equation (18), performed by block 6, Fig. 4, is provided by the subsystem of the Simulink model of the distributed cable line with active-inductive load (Fig. 6, a). Blocks B1–B4 set the matrix coefficients  $\mathbf{B}_1$ – $\mathbf{B}_4$  according to expressions (19)–(22). Integrator2 integrates the right side of equation (18). A zero vector comes to the input  $x_0$  of initial conditions. The output of the subsystem shows the calculated values of the  $\mathbf{X}$  vector for the current point in time.

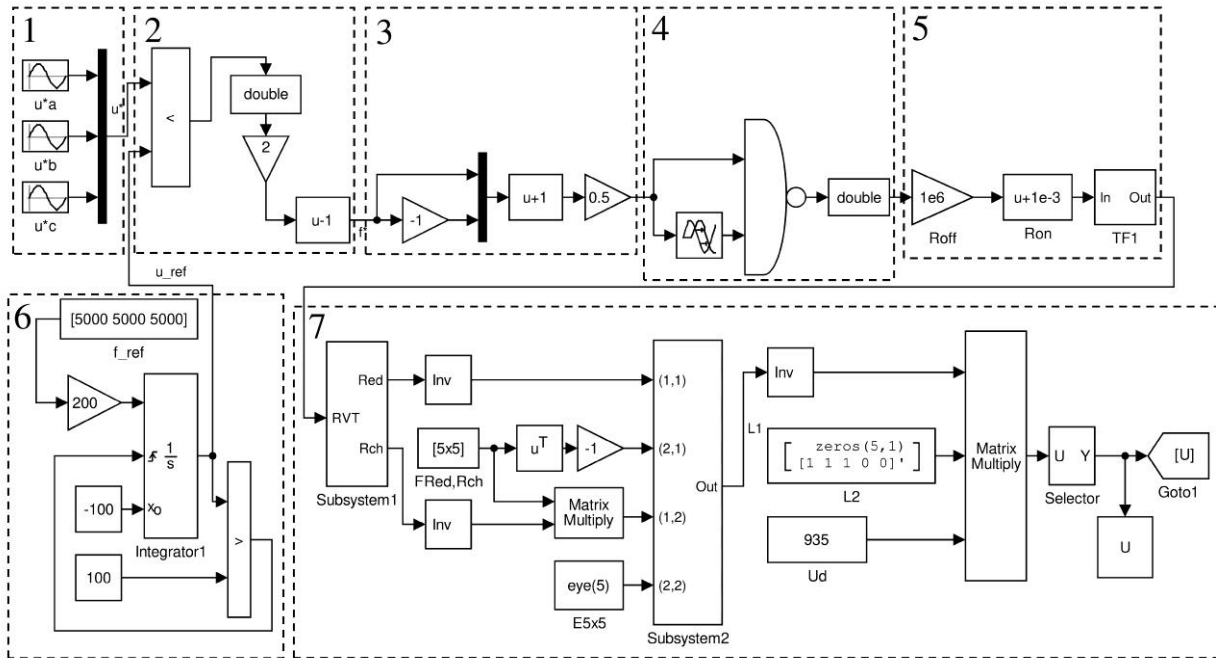


Fig. 5. Simulink subsystem of the autonomous voltage inverter, compiled according to equation (8), with the subsystem of PWM control signals generation

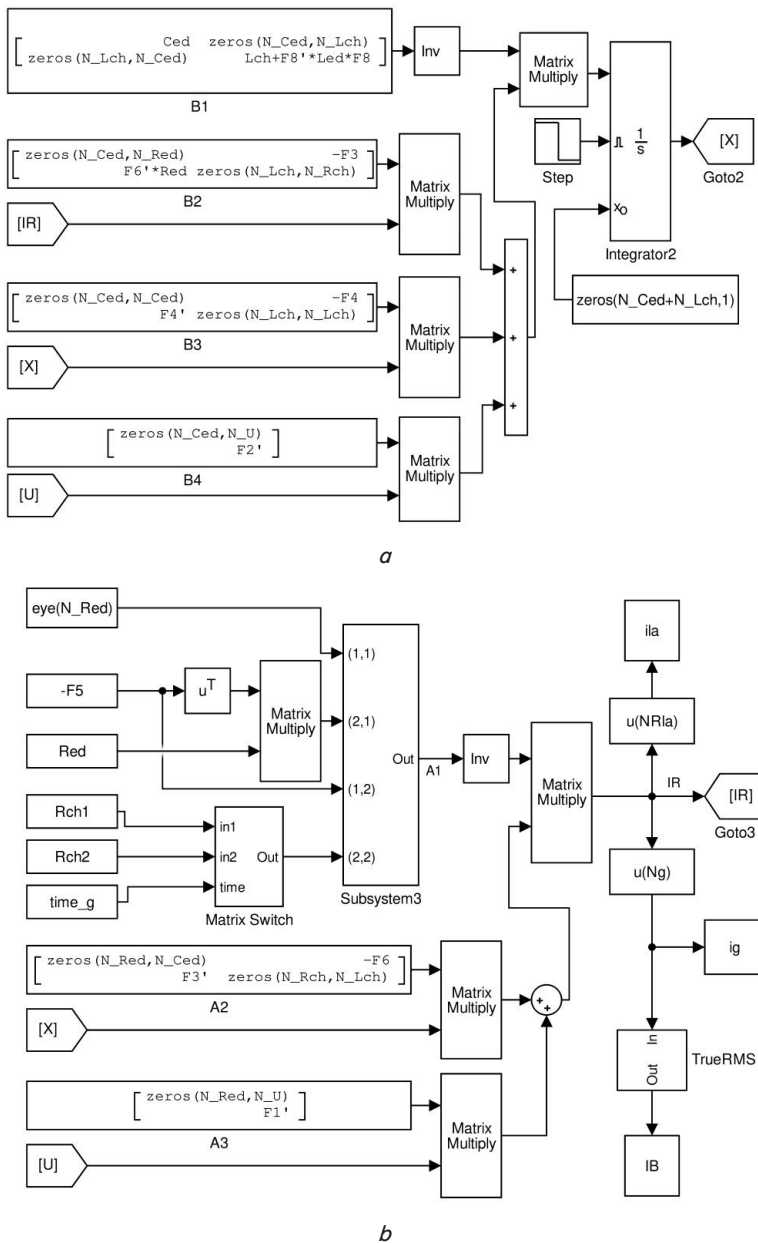


Fig. 6. Simulink model of the distributed cable line with active-inductive load: *a* – subsystem that solves the matrix differential equation (18) of state; *b* – subsystem that calculates the vector  $I_R$  of resistive elements currents according to (13)

The subsystem of Simulink model, shown in Fig. 6, *b*, performs the calculation of the  $I_R$  vector according to (13) and the equivalent current  $I_B$  through the human body (Fig. 4, blocks 7 and 8, respectively). The Rch1 and Rch2 blocks correspond to the resistivity chord matrices before and after the point  $t_g$  in time (given by the time\_g block), when the ground fault occurs. The value of the resistive chords matrix, which corresponds to the current point in simulation time, is taken into account in the matrix coefficient  $A_1$  (14) by the Matrix Switch. The coefficient  $A_1$  is formed by Subsystem3. The matrix coefficients  $A_2$  and  $A_3$ , according to expressions (15) and (16), are given by blocks A2, A3. The instantaneous values of the  $I_R$  vector are formed at the output of the subsystem. Block  $u(Ng)$  distinguishes from  $I_R$  the instantaneous values of the ground fault current

in the elementary section with the  $N_g$  number. The TrueRMS block provides the calculation of the equivalent current  $I_B$  value through the human body at industrial frequency.

Thus, the proposed subsystems (Fig. 5, 6) of the Simulink model of the frequency converter cable branch make it possible to determine the ground fault current.

### 7. Practical recommendations for increasing the electrical safety of underground electrical networks equipped with frequency converters

It is possible to increase the operational electrical safety of FC cable branches of power networks with isolated neutral point by applying the method of insulation resistance monitoring of the power network branch equipped with the semiconductor frequency converter [13]. The principle of control is explained by the diagram in Fig. 7. The power switch 1 supplies FC 2, which includes rectifier 3, capacitance filter 4 and AVI 5. To the output of the frequency converter 2 using cable 6, the insulation of which is characterized by resistors 7, the load 8 is connected. Each phase of the latter is characterized by inductance 9 and resistance 10.

The device 11 that implements the monitoring method includes a measuring circle, which consists of: inductor 12; sensor 13 of instantaneous values of the measuring current; additional source 14 of constant measuring voltage; ground connection 15. Sensor 16 of instantaneous values of the measuring voltage, applied to the branch, is also used. Analog-to-digital converters 17, 18 and digital filters 19, 20 are connected to the outputs of sensors 13, 16, respectively. The latter distinguish a constant component of the signals that are proportional to the instantaneous values of the measuring current and voltage. The obtained values come to the inputs of the block 21 that calculates the insulation resistance of the cable branch. The obtained value is compared by the block 22 with the setpoint of the branch insulation resistance, which comes from the block 23. The signal from the comparison block 22 output is transmitted to switch off the branch of the electrical network. The specified signal equals a logical "1" if the actual insulation resistance is less than the specified setpoint. The signal equals a logical "0" if the actual insulation resistance exceeds the specified setpoint.

Thus, the possibility of detecting the insulation resistance decrease is achieved by distinguishing the constant components of the measuring voltage and current and by controlling their ratio. The result does not depend on the operation mode of the frequency converter. The signal to deenergize the power network branch is generated in case of emergency mode detection. This increases the electrical safety of the frequency converter cable branch.

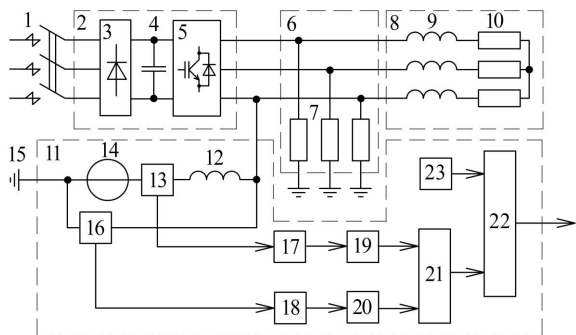


Fig. 7. Circuit diagram of the electrical network with the FC and device for insulation resistance monitoring of the power network branch

### 8. Discussion of the results of single phase-to-ground fault simulation in the frequency converter cable branch

A fragment of the 660 V power network of coal mine section is selected for numerical analysis. The neutral point of the secondary winding of the power transformer is isolated. The starting unit, equipped by the FC of PRCh-400M type is utilized. The latter is equipped with the Danfoss VLT Automation Drive FC-302 N400T7 frequency converter with a 400 kW power output. An induction motor VAO5P560S6, rated power 400 kW, is connected to the FC using a 300 m long BiTmining NSSHCOEU 3×150+3×70/3 cable. The cable line was conditionally divided into  $N=100$  elementary sections. The frequency of the inverter output voltage is  $f=50$  Hz, the PWM reference frequency  $f_{ref}=5$  kHz. The voltage of FC direct current circuit  $U_d = 3\sqrt{6}U_{lg} / \pi = 935$  V is determined according to the phase voltage  $U_{lg}=400$  V at the rectifier input in the idle mode.

The graph of the equivalent circuit of the cable branch with active-inductive load has the following quantitative characteristics: branches – 1.209; nodes – 609; independent voltage sources – 3; capacitive edges – 300; resistive edges – 303; inductive edges – 2; resistive chords – 300; inductive chords – 301. The parameters of the  $\Delta l=3$  m long cable elementary section of the accepted type are:  $R_{ccj}=3.96 \cdot 10^{-4} \Omega$ ;  $L_{ccj}=8.70 \cdot 10^{-7}$  H;  $R_{gcj}=3.33 \cdot 10^8 \Omega$ ;  $C_{gcj}=1.35 \cdot 10^{-9}$  F. The parameters values of the active-inductive load with a power of 400 kW at a power factor of 0.9 are:  $R_{lc}=1.086 \Omega$ ;  $L_{lc}=1.7$  mH. The case of phase A ground fault in the elementary section  $N_g=50$  of the cable through a human body with resistance of 1 k $\Omega$  was considered. Numerical simulation is performed in Simulink using the trapezoidal interpolation method (ode23t solver), and the integration step does not exceed  $1 \cdot 10^{-5}$  s. Dynamic processes in the system for 50 ms are simulated.

As a result of the ground fault simulation in the FC cable branch under the given equipment parameters, the following graphs are obtained. The graph of the instantaneous values of AVI output phase voltage is illustrated by Fig. 8, of instantaneous values of the load phase current – by Fig. 9. The graph (Fig. 10) of instantaneous values of ground fault current through the human body in case of such emergency at the point  $t_1=11$  ms in time was also obtained. Fragments of these graphs (Fig. 7–9), corresponding to the time interval from  $t_2=25.6$  ms to  $t_3=26.6$  ms, are shown in Fig. 10–12, respectively, at a large scale.

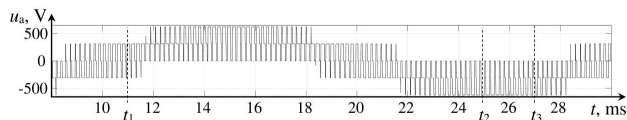


Fig. 8. Graph of the instantaneous values of AVI output phase voltage as a function of time  $t$ , obtained from simulation

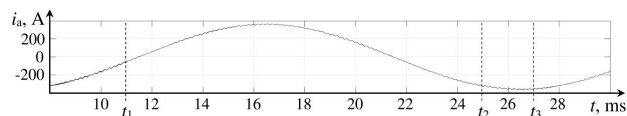


Fig. 9. Graph of instantaneous values of the load phase current in FC cable branch as a function of time  $t$ , obtained from the simulation

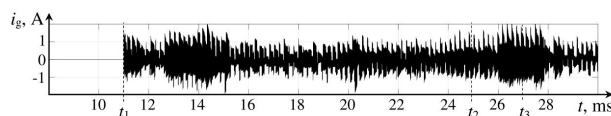


Fig. 10. Graph of instantaneous values of ground fault current through the human body as a function of time  $t$ , obtained from the simulation

As can be seen from the graphs, a single side PWM voltage is applied to the cable (Fig. 8). The discrete voltage form (Fig. 11) is smoothed out by the reactivity of the cable and the form of load current approaches the sinusoidal (Fig. 9). The higher harmonics amplitudes of the load current curve are significantly smaller than the amplitude of the first harmonic (Fig. 12).

The resistance of  $R_{ga50}$  is discretely reduced to a value of the human body resistance, 1 k $\Omega$ , if the insulation damage of the elementary section  $N_g=50$  occurs at point  $t_1$  in time. Accordingly, the current through the specified resistance increases (Fig. 10). This current corresponds to the ground fault current through the human body. The current has a polyharmonic composition and consists of fragments, each of which corresponds to the conduction intervals of the AVI power keys pair of the damaged phase (Fig. 13). The peak values of the current through the human body reach 2 A.

The calculated equivalent value of current at industrial frequency through the human body is  $I_B=0.51$  A. According to the IEC 60479-1 standard, the probability  $P_{vf}$  of ventricular fibrillation occurrence depends on the magnitude of  $I_B$  current and  $t_B$  duration of its flow. For the obtained  $I_B$  value at  $t_B < 200$  ms, the probability  $P_{vf}$  is about 0.05. At  $500 \text{ ms} < t_B < 200$  ms, the probability  $P_{vf} \approx 0.5$ . If the current flow time  $t_B > 500$  ms, then  $P_{vf} > 0.5$ .

The obtained data illustrate that the occurrence of ground fault through the human body in the FC cable branch of a given network is characterized by an unacceptably high probability of ventricular fibrillation. The calculated probability value of 0.05 with a current duration of up to 200 ms significantly exceeds the maximum permissible probability ( $1 \cdot 10^{-6}$ ) of the specified state. Such circumstance emphasizes the necessity of applying the proposed method to increase the electrical safety of underground electrical networks with isolated neutrals equipped with frequency converters.

The results of the study were obtained by ignoring the insulation parameters of the cable that connects the FC to the substation. Also, the dependence of the body resistance

on the applied contact voltage and the skin capacity at the point of contact were not taken into account.

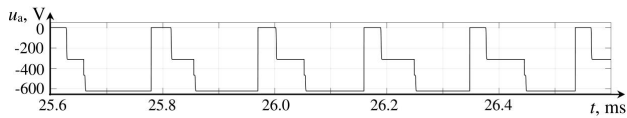


Fig. 11. Graph of the instantaneous values of AVI output phase voltage over the time interval ( $t_2$ ,  $t_3$ ) according to Fig. 8

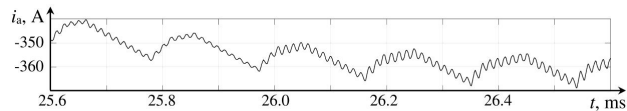


Fig. 12. Graph of instantaneous values of the load phase current in the FC cable branch over the time interval ( $t_2$ ,  $t_3$ ) according to Fig. 9

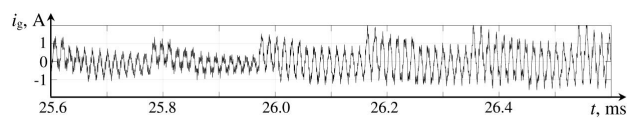


Fig. 13. Graph of instantaneous values of ground fault current through the human body over the time interval ( $t_2$ ,  $t_3$ ) according to Fig. 10

Follow up studies will be focused on analyzing the mode of single phase-to-ground fault in the power network of the mine section, which includes several frequency converters with cable branches.

## 9. Conclusions

1. The mathematical model of autonomous voltage inverter in the frequency converter as a part of the mine section power network is improved. The model differs from the known ones by taking into account the discrete nature of the converter output voltage and the inertia of the power

semiconductor devices switching, which specifies the shape of the voltage curve at the converter output.

2. The method for forming a mathematical model of a three-phase cable line with distributed parameters as a set of differential equations of state and algebraic equations in matrix form is proposed. There are no restrictions on the number of three-phase elementary sections that are distinguished in the cable line during the analysis. The method allows to take into account the wave processes in the cable under the effect of high-frequency pulse-width modulated voltage. The asymmetry of insulation phase-to-ground resistances that accompanies the ground fault is also taken into account. The use of the matrix-topological method for analysis improves the efficiency of numerical simulation by avoiding operations with partial derivatives with respect to geometric coordinates of the cable.

3. The structure of the computer model of the FC cable branch in case of ground fault is substantiated. The model enables dynamic processes to be analyzed in the long cable branch of the frequency converter. Numerical interpolation trapezoid method is used to integrate the differential equations. This takes into account the distributed parameters of the cable and the significant transverse asymmetry that accompanies the single phase-to-ground fault. This approach allows to obtain instantaneous values of the ground fault current at an arbitrary point of the cable line and to estimate the probability of fatal electrocution.

4. The method of insulation resistance monitoring of the power network branch equipped with the semiconductor frequency converter is substantiated. The implementation of the method will improve the electrical safety of underground electrical networks by timely detection of isolation damage in the FC cable branch and transmission of the signal to deenergize the electrical network.

5. The unacceptably high probability of ventricular fibrillation is established for the network of specified configuration as a result of numerical simulations in case of ground fault through a human body in the FC cable branch. The calculated probability value of 0.05 with a current duration of up to 200 ms significantly exceeds the maximum permissible probability ( $1 \cdot 10^{-6}$ ) of the specified state.

## References

- Ravlić, S., Marušić, A., Havelka, J. (2017). An improved method for high impedance fault detection in medium voltage networks. *Technical gazette*, 24 (2), 391–396. doi: <https://doi.org/10.17559/tv-20151012082303>
- Wymann, T., Pollock, M., Rees, J. (2015). A new approach to mining earth leakage protection with medium voltage drives. *Industrial-Electrix*, 24–27. Available at: <https://www.littelfuse.com/~media/protection-relays/articles/el731-industrial-electrix-article-2015-2.pdf>
- Marek, A. (2017). Influence of indirect frequency converters on operation of central leakage protection in underground coalmine networks. *Mining - Informatics, Automation and Electrical Engineering*, 3 (531), 9–20. doi: <https://doi.org/10.7494/miag.2017.3.531.9>
- Hafner, A. A., Ferreira da Luz, M. V., Carpes, Jr. W. P. (2015). Impedance and admittance calculations of a three-core power cable by the finite element method. *International Conference on Power Systems Transients*. doi: <http://doi.org/10.13140/RG.2.1.4873.5848>
- Shanmugasundaram, N., Vajubunnisa Begum, R. (2017). Modeling and Simulation Analysis of Power Cables for a Matrix Converter Fed Induction Motor Drive (MCIMD). *Journal of Advanced Research in Dynamical and Control Systems*, 11, 734–744. Available at: <http://jardcs.org/papers/v9/sp/6359.pdf>
- Hoshmeh, A., Schmidt, U. (2017). A Full Frequency-Dependent Cable Model for the Calculation of Fast Transients. *Energies*, 10 (8), 1158. doi: <https://doi.org/10.3390/en10081158>
- Czaja, P. (2016). Anti-shock safety of industrial electric installations with built-in frequency converters. *2016 Progress in Applied Electrical Engineering (PAEE)*. doi: <https://doi.org/10.1109/paee.2016.7605113>
- Czapp, S., Borowski, K. (2013). Immunity of Residual Current Devices to the Impulse Leakage Current in Circuits with Variable Speed Drives. *Electronics and Electrical Engineering*, 19 (8). doi: <https://doi.org/10.5755/j01.eee.19.8.2883>



9. Cocina, V., Colella, P., Pons, E., Tommasini, R., Palamara, F. (2016). Indirect contacts protection for multi-frequency currents ground faults. 2016 IEEE 16th International Conference on Environment and Electrical Engineering (EEEIC). doi: <https://doi.org/10.1109/eeeic.2016.7555701>
10. Czapp, S., Guzinski, J. (2018). Electric shock hazard in circuits with variable-speed drives. Bulletin of The Polish Academy of Sciences: Technical Sciences, 66 (3), 361–372. doi: <http://doi.org/10.24425/123443>
11. Czapp, S. (2010). The effect of PWM frequency on the effectiveness of protection against electric shock using residual current devices. 2010 International School on Nonsinusoidal Currents and Compensation. doi: <https://doi.org/10.1109/isncc.2010.5524515>
12. Syvokobylenko, V. F., Vasylets, S. V. (2017). Matematychnе modeliuвання perekhidnykh protsesiv v elektrotekhnichnykh kompleksakh shakhtnykh elektrychnykh merezh. Lutsk: Vezha-Druk, 272.
13. Pat. No. 135438 UA. Sposib kontroliu aktyvnoho oporu izoliatsiyi vidhaluzhennia elektrychnoi merezhi z napivprovodnykovym peretvoriuvachem chastoty (2019). MPK6 G01R 27/18, H02H 3/16. No. u201901598; declared: 18.02.2019; published: 25.06.2019, Bul. No. 12.

Проведено порівняльний аналіз результатів оцінювання відповідності програмного забезпечення (ПЗ) для засобів виміральної техніки (ЗВТ). Для порівняльного оцінювання обрано вісім ПЗ ЗВТ з вмонтованим та універсальним комп'ютерами. Обрані ПЗ ЗВТ попередньо пройшли оцінювання за методиками та алгоритмами, які базуються на вимогах національних стандартів та документів міжнародних і регіональних організацій законодавчої метрології OIML та WELMEC. За результатами проведеного аналізу вимог настанови WELMEC щодо випробування ПЗ ЗВТ були виділені узагальнені та часткові показники для оцінювання якості ПЗ ЗВТ. Сформовано вирази для отримання чисельного значення кожного часткового показника за кожним узагальненим показником.

Для порівняльного оцінювання обрано метод аналітичної ієрархії (МАІ), оскільки він дозволяє порівняти і виконати кількісну оцінку альтернативних варіантів рішення. З метою релевантного порівняння під час оцінювання конкретного ПЗ ЗВТ були враховані всі порівнювані елементи. Останні були згруповані в узагальнені показники, кожен з яких оцінено окремо. Попарні порівняння й усі інші етапи оцінювання з використанням МАІ виконувались на основі узагальнених показників. Для попарного порівняння всіх кількісних та якісних показників з поданням результату зрівняння у кількісній формі, було використано шкалу Сааті. Експертним методом визначено коефіцієнти ваги кожного часткового показника.

Визначено основні показники для ПЗ ЗВТ з вмонтованим та універсальним комп'ютером, які мають найбільший вплив на результати оцінювання відповідності. Встановлено, що без представлення документації та ідентифікації ПЗ ЗВТ з вмонтованим та універсальним комп'ютерами неможливо розпочинати процедуру оцінювання відповідності згідно з вимогами. Показник перевірки запам'ятовуючих пристроїв та спеціальний показник перевірки ПЗ для певного ЗВТ є одними із вагомих показників. У той же час показники перевірки зчитування та перевірки рівнів розділення ПЗ практично не застосовні і ними можна знехтувати.

Ключові слова: програмне забезпечення, засіб виміральної техніки, оцінювання якості, метод аналізу ієрархій

UDC 389:14:621.317:354

DOI: 10.15587/1729-4061.2019.175811

# QUALITY ASSESSMENT OF MEASUREMENT INSTRUMENT SOFTWARE WITH ANALYTIC HIERARCHY PROCESS

O. Velychko

Doctor of Technical Sciences, Professor, Director  
Scientific and Production Institute of  
Electromagnetic MeasurementsState Enterprise "All-Ukrainian State Scientific and Production  
Centre for Standardization, Metrology, Certification and  
Protection of Consumer",  
(SE "Ukrmetrteststandard")

Metrolohychna str., 4, Kyiv, Ukraine, 03143

O. Hrabovskyi

PhD, Associate Professor, Director

Educational and Scientific Institute of Metrology, Automation,  
Intellectual Technologies and Electronics\*

T. Gordiyenko

Doctor of Technical Sciences,

Professor, Head of Department

Department of Standardization, Conformity Assessment and  
Educational Measurements\*

E-mail: t\_gord@hotmail.com

\*Odessa State Academy of

Technical Regulation and Quality

Kovalska str., 15, Odessa, Ukraine, 65020

Received date 10.06.2019

Accepted date 25.07.2019

Published date 28.08.2019

Copyright © 2019, O. Velychko, O. Hrabovskyi, T. Gordiyenko

This is an open access article under the CC BY license

<http://creativecommons.org/licenses/by/4.0>

## 1. Introduction

The requirements of the Measuring Instruments Directive 2014/32/EU (MID) [1] form the basis of the legislation

of Ukraine on conformity assessment of measuring instruments (MI). According to the new version of the Law of Ukraine "On metrology and metrological activity" (came into force on 01.01.2016), MI intended for application in